Defect clusters in hexagonal networks: characterization and strain field

1998 J. Phys.: Condens. Matter 10 7519

(http://iopscience.iop.org/0953-8984/10/34/006)

J. Phys.: Condens. Matter **10** (1998) 7519–7534. Printed in the UK PII: S0953-8984(98)91638-1

Defect clusters in hexagonal networks: characterization and strain field

M A Fortes and M Fátima Vaz

Departamento de Engenharia de Materiais, Instituto Superior Técnico Av. Rovisco Pais, Lisboa, Portugal

Received 13 February 1998, in final form 15 May 1998

Abstract. A detailed analysis of defect clusters (topological and geometrical) in hexagonal networks is presented. The conditions that have to be met by a cluster for it to be embedded in an hexagonal network are enunciated, which are related to the sequence of saturated (3-connected) and unsaturated (2-connected) vertices at the periphery of the cluster (vertex sequence). The type of hexagonal network (perfect, dislocated or disclinated) in which a defect is embedded depends on simple parameters (the strength P of the cluster and a Burgers vector $\boldsymbol{B}$ for dislocation clusters) which can be obtained from the vertex sequence. Equivalent clusters can be embedded in hexagonal networks of the same topology and equivalence classes are identified for all types of clusters.

Disclination defects of given strength, P ($P \neq 0$), may fill into one or more classes, depending on P. For dislocation defects ($P = 0$) there are infinitely many classes, each defined by a vector $\boldsymbol{B}$. The strain field and strain energy density in the hexagonal network around a single defect cluster is evaluated for geometrical and topological defects of any type, using a continuum approach.

1. Introduction

In the study of cellular systems, typified by liquid or solid foams and polycrystals, it is usual to consider two extreme types of structures, namely, completely ordered with identical cells, and completely disordered or random with cells of different sizes and shapes (see, for example, Weaire and Rivier [1]). In two-dimensional (2D) cellular systems with trivalent vertices (three edges at each vertex) the simplest ordered structure is the hexagonal network or honeycomb, formed by identical regular hexagonal cells. Random 2D cellular systems have cells with a distribution of areas and number of sides, i (equal to the number of neighbours). An intermediate degree of order in a 2D network can be achieved by introducing defects in an originally perfect honeycomb. The network in which the defects are embedded is hexagonal, but the cells are no longer regular hexagons because of the strain due to the defects. The defects to be considered can be classified as point defects as distinct from line defects (grain boundaries) which separate two hexagonal networks. We discuss only isolated defects, leaving the problem of defect interaction for future research.

The central question that will be discussed is as follows. What conditions must a defect cluster satisfy for it to be possible to surround the cluster with hexagonal cells, which form an (unbounded) hexagonal network? These conditions are purely topological. The area of the cluster and the areas of its individual cells can be changed at constant topology without changing the area A_0 of the surrounding hexagonal cells.

0953-8984/98/347519+16$19.50

The discussion in this paper therefore concentrates on topological properties of clusters and we may admit that all cells (the cluster cells and the surrounding cells) have the same area. Geometrical effects appear only when the strain field of a defect is considered, and will be discussed at the end of the paper.

Isolated defects in honeycomb soap froths have been the object of some recent theoretical [2–4] and experimental studies [5–7]. A defect grows by invading the surrounding honeycomb and randomizing it. The effect of defects on the mechanical properties of solid honeycombs has also received attention in recent years (e.g. [8]).

Defects in periodic media is of course a subject that has attracted enormous attention in the literature. However, the application of this basic knowledge to defects in cellular structures is rather limited. Morral and Ashby [9] discussed in detail a particular type of defect—a pair of 5- and 7-sided cells—in a honeycomb. Those authors also referred to other simple defects (e.g. a 4/8 pair) but did not discuss more general ones. The 5/7 pair is a dislocation that plays an important role in the deformation of a honeycomb froth [10]. More complex defects with dislocation character were produced by the present authors in a honeycomb froth [5] while Harris [11] produced one cell disclinations in a froth.

The plan of the paper is as follows. We first introduce in section 2 simple definitions related to the topology of defect clusters, namely, the vertex sequence and the strength P of a cluster. In section 3 we give the conditions that a cluster must satisfy to be embedded in an hexagonal network. The definition and properties of six-belts of clusters are introduced in section 4, leading to the definition of equivalent clusters and equivalent six-belts. In section 5 we give simple rules to obtain the b-circuit (Burgers circuit) of a cluster from its vertex sequence. In section 6 we classify the clusters into various types (neutral, dislocations and disclinations) and identify the equivalence classes of clusters. The concept of topological size of a cluster is introduced in section 7. Finally, section 8 deals with the strain field and strain energy density of topological and geometrical defects.

2. Vertex sequence and power of a cluster

At the periphery of a cluster of cells we distinguish between unsaturated and saturated vertices, with respectively two and three edges of the cluster connected at them. These vertices are marked by (o) and (·), respectively, in the cluster of figure 1(a). Dangling edges (d-edges) can be connected at the (o)-vertices. The total numbers of (o) and (·)-vertices at the periphery of a cluster are u and s, respectively. The number of peripheric edges of the cluster is p with

$$p = u + s. \tag{1}$$

The average number, $\bar{n}_c$, of sides per separated cell of the cluster is given by (e.g. [12])

$$\bar{n}_c = 6 - \frac{6 + p - 2u}{N_c} = 6 + \frac{u - s - 6}{N_c} \tag{2}$$

where N_c is the number of cells in the cluster. For each cluster we define the number P, called the strength of the cluster, as

$$P = u - s - 6. \tag{3}$$

The average number $\bar{n}_c$ of sides per separated cell is then

$$\bar{n}_c = 6 + \frac{P}{N_c}. \tag{4}$$

The sequence of (o) and (·)-vertices at the periphery of a cluster will be termed the vertex sequence of the cluster. It can be displayed by marking the successive vertices around a circle, as in figure 1(b). A line representation as in figure 1(c) can also be used noting that the extremes of the line are, in fact, adjacent. Finally, a numerical representation, formed by the (cyclic) sequence of the numbers n_0 of unsaturated (o)-vertices between successive (·)-vertices, provides a more condensed representation of the vertex sequence; an example is given in figure 1(c). In this representation the number of entries n_0 is s and the sum of all entries is u. Therefore, $P + 6$ equals the sum of the s numbers $(n_0 - 1)$.

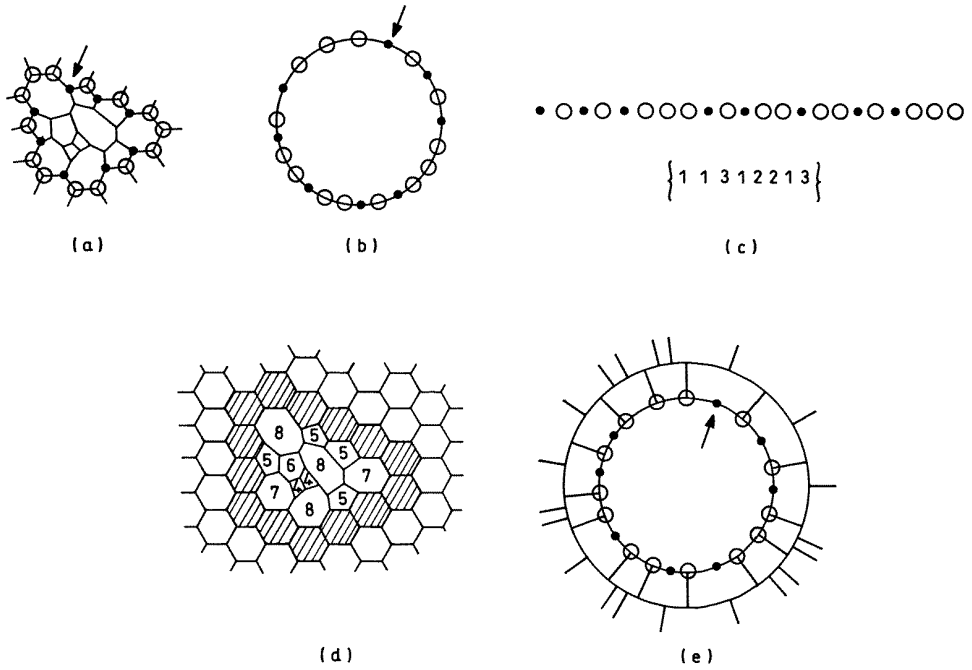

Figure 1. (a) A defect cluster with $N_c = 12$ cells, $s = 8$ saturated (·)-vertices and $u = 14$ unsaturated (o)-vertices. (b) The vertex sequence is displayed on a circle or (c) on a line diagram. The numerical sequence of vertices is also indicated in (c). The cluster can be embedded in an hexagonal network, as shown in (d) where the short six-belt is formed by the shaded cells. In (e) is shown a simplified drawing of the cluster short six-belt. The arrow indicates a starting point for the vertex sequence shown in (c).

As hexagonal cells are connected at the periphery of the cluster, the vertex sequence changes. The transformations that can occur as one hexagon is added to expand the cluster are of the following types, as regards the changes that they originate locally in the vertex sequence (see figure 2)

$$\begin{aligned} \text{o}\cdot\cdot\cdot\cdot\text{o} &\rightarrow \quad \cdot\cdot \qquad \text{Op1} \\ \text{o}\cdot\cdot\cdot\text{o} &\rightarrow \quad \cdot\text{o}\cdot \qquad \text{Op2} \\ \text{o}\cdot\cdot\text{o} &\rightarrow \quad \cdot\text{o}\,\text{o}\cdot \qquad \text{Op3} \\ \text{o}\cdot\text{o} &\rightarrow \quad \cdot\text{o}\,\text{o}\,\text{o}\cdot \qquad \text{Op4}. \end{aligned} \tag{5}$$

The quantity P is conserved in all these operations. The reverse of operations (5), which will be indicated by Op $\bar{1}$, etc, can be used to remove any peripheric six-cells that a cluster may have in order to obtain a proper defect cluster.

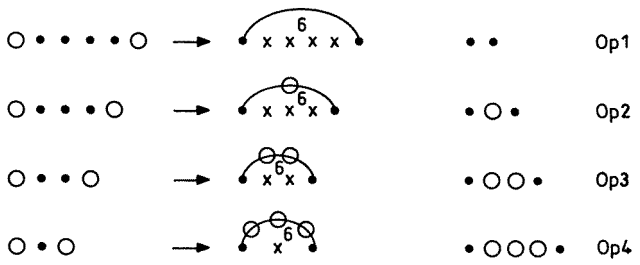

Figure 2. Operations Op1 to Op4 of the addition of an hexagonal cell at the periphery of a cluster. The original (·)-vertices are marked with crosses in the final state.

3. Embeddable clusters

The problem that we wish to address can be stated as follows (see figure 1). Given a 2D cluster of interconnected cells, can it be incorporated in an hexagonal network, that is, can it be surrounded by successive shells of hexagonal cells? We refer to these clusters as embeddable clusters. The cluster of figure 1(a) can be embedded in an hexagonal network as shown in figure 1(d) and, in a simpler representation, in figure 1(e). Three conditions have to be met for a cluster to be embeddable.

1. The cluster has at least three (o)-vertices:

$$u \geqslant 3. \tag{6}$$

This condition is generally required for a cluster to be surrounded by cells with a number of vertices $i \geqslant 3$ (convex networks).

2. As hexagonal cells are placed around the cluster, through successive operations of types Op1 to Op4, defined earlier, the number of (o)-vertices does not increase except in Op4. If hexagonal cells (of constant area A_0) are to be placed indefinitely, the number of (o)-vertices has to increase, that is, at all stages $u - s > 0$; otherwise the average tangential linear dimension of six-cells would increase as new six-cells are added around the cluster. Since the difference $u - s = P + 6$ is invariant, we conclude that an embeddable cluster must have

$$P \geqslant -5. \tag{7}$$

If $u = s$ as in figure 3 hexagons can be placed indefinitely, but since the number of (o)-vertices does not increase in successive shells, the average angular width of the hexagons will remain constant. We do not consider clusters with $P < -5$.

3. There are particular subsequences of (o) and (·) vertices in the vertex sequence which forbid the insertion of successive hexagons. For example, the subsequence

$$\mathrm{o} \cdot \cdot \cdot \cdot \cdot \mathrm{o}$$

with five successive (·)-vertices does not permit the insertion of an hexagon, as shown in figure 4(a). This sequence is indicated by {5}. Other forbidden subsequences are those that inevitably lead to five or more successive (·)-vertices when hexagons are added (i.e. in whatever order or location the hexagons are placed, five or more successive (·)-vertices will appear). This means that the forbidden subsequences are those that can be obtained from {5} by the reverse operations $\mathrm{Op}\bar{1}$ to $\mathrm{Op}\bar{4}$. Using this method, it is possible to enumerate all forbidden subsequences derived from {5}. Examples are

$$\{043\}\ \{142\}\ \{332\}\ \{1331\}\ \{03231\}\ \{12321\}\ \{0304031\}\ \{0222221\}. \tag{8}$$

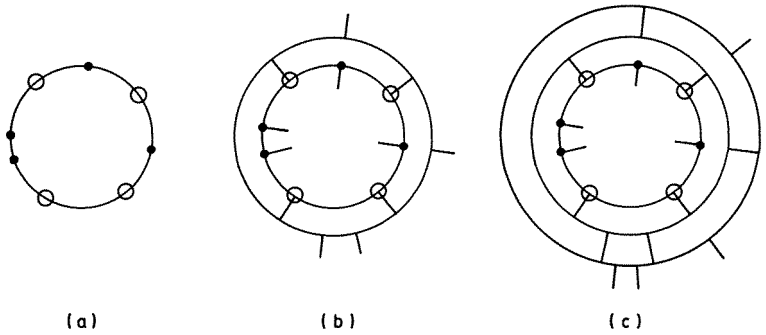

Figure 3. The vertex sequence shown in (a) has $u = s$ and is surrounded by successive layers of hexagons as in (b) and (c). However, the number of hexagons in successive layers remains constant, implying that their average peripheric length increases indefinitely.

In figure 4(b) is shown the forbidden sequence {043}.

Forbidden subsequences are derived from {5} through operations that leave $(u - s)$ unchanged. Subsequences with more $(\cdot)$-vertices are of course also forbidden. Forbidden subsequences are thus of the form

$$\{a_1 a_2 \dots a_n\} \qquad \text{with} \qquad \sum_{i=1}^{n}(a_i - 1) \geqslant 4. \tag{9}$$

However, this condition is not sufficient for a subsequence to be forbidden. For example {33} and {42} are permitted subsequences as shown in figure 4(c) for {42}.

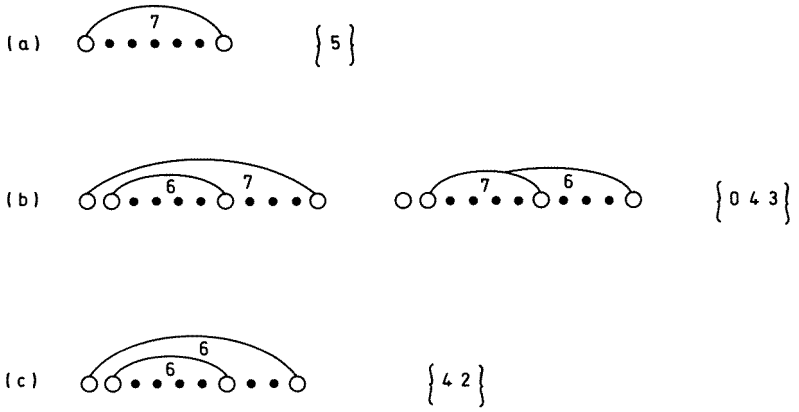

Figure 4. (a, b) Examples of vertex subsequences to which hexagonal cells cannot be added. Both have $n(\cdot) - n(\mathrm{o}) = 3$. However, the subsequence {42} in (c) with the same difference $n(\cdot) - n(\mathrm{o}) = 3$ can accommodate hexagons.

In conclusion, embeddable clusters have $u \geqslant 3$, $u > s$ (or $P \geqslant -5$) and no subsequences such as (8) which can be derived from $\{n\}$ with $n \geqslant 5$.

4. Six-belts and equivalence of clusters

The first complete shell of connected hexagons around an embeddable cluster will be termed the cluster short six-belt. Other shells of this type encircling the defect are termed six-belts. The short six-belt of the cluster of figure 1(a) is formed by the hatched cells of figure 1(d). All cells in and outside any six-belt are, of course, hexagons. Another example of a short six-belt is in figure 5(a), with the dangling edges (*d*-edges) of the six-belt drawn at the outer periphery of the belt. In this and other drawings, the hexagons are represented in successive concentric shells (see also figure 1(e)). Each hexagon of a six-belt is connected to two other hexagons in such a way that no more than two six-cells of the belt meet at a vertex. The six-cells of the belt therefore have, at most, two (o)-vertices (two *d*-edges). Six-cells with three or four (o)-vertices, such as in figure 6, need not and will not be used in six-belts.

The vertex sequence of a cluster completely determines the topology (or arrangement) of the hexagons around the cluster. If hexagons are added to the cluster at its periphery another cluster is obtained which is embeddable in the same network. The two clusters, their vertex sequences and six-belts are said to be equivalent. Equivalent vertex sequences can be obtained by using the operations Op1 to Op4 previously defined (equation (5)) by

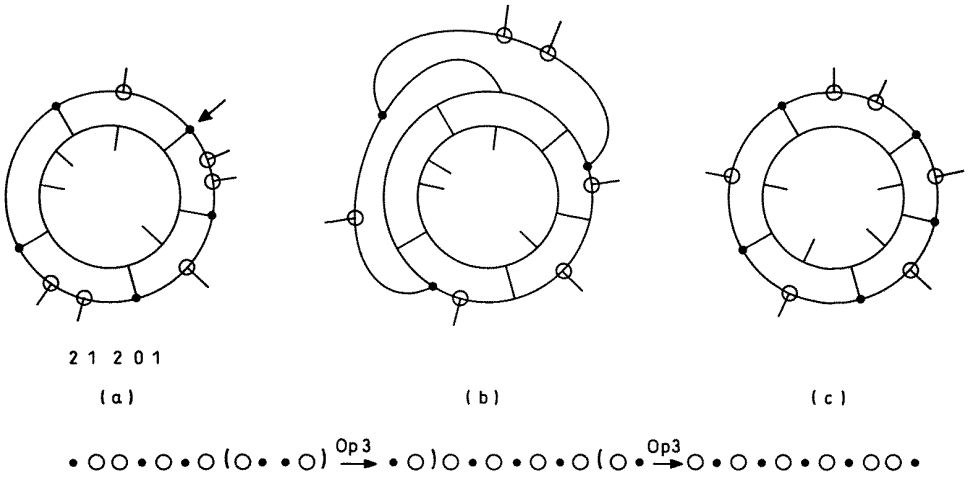

Figure 5. The six-belt in (a) is transformed into a standard six-belt shown in (c) by the addition of two successive hexagons, as indicated in (b) and in the numerical representation at the bottom.

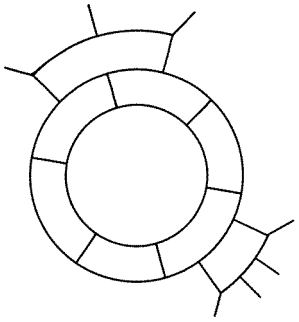

Figure 6. Hexagonal cells with three or four dangling edges are excluded from six-belts.

the addition of hexagons at the periphery of a cluster. Clearly the reverse operations can also be used to transform a vertex sequence into an equivalent one.

We will now show that given a vertex sequence it is possible to find an equivalent vertex sequence with entries 1 and 2 only, that is, such that: (a) the number of successive (o)-vertices is at most 2 and (b) there are no successive (·)-vertices. Such a vertex sequence (for example {12212221}) will be termed a standard vertex sequence. The number of entries 2 is $P + 6$.

Given an arbitrary vertex sequence (e.g. the one of figure 5(a)), an equivalent standard sequence can be obtained by first eliminating subsequences of two, three or four successive (·)-vertices by means of operations Op1 to Op3 defined in (5). This procedure is exemplified in figure 5(b) and leads to the vertex sequence in figure 5(c). Next, any subsequences with three or more (o)-vertices are fragmented using the following rule

$$\text{o} \cdot \text{ooo} \cdot \text{o} \rightarrow \cdot\text{oo} \cdot \text{oo} \cdot \text{oo} \cdot \text{oo} \cdot$$
$$\text{o} \cdot \text{ooo} \cdot \text{o} \rightarrow \cdot\text{oo} \cdot \text{oo} \cdot \text{oo} \cdot \text{oo} \cdot \text{oo} \cdot \quad \text{etc}$$

in which n successive (o)-vertices are replaced by $(n + 1)$ pairs (o o) separated by one (·)-vertex. This rule results from the application of successive Op4 operations and a final Op3.

To a standard vertex sequence we may associate a standard six-belt which is a six-belt for which the vertex sequence at its outer periphery is that standard sequence. Figure 5(c) shows an example of a standard six-belt.

In conclusion, we may characterize a cluster by a standard vertex sequence or a standard six-belt, which are equivalent to the vertex sequence of the cluster and to its short six-belt, respectively, in the sense that a unique network of hexagons around the defect is determined by them.

5. The *b*-circuit

In the hexagonal lattice of the perfect and regular honeycomb we take three primitive vectors $\boldsymbol{b}_1\boldsymbol{b}_2\boldsymbol{b}_3$ in the clockwise sequence (figure 7). We have

$$\boldsymbol{b}_1 + \boldsymbol{b}_2 + \boldsymbol{b}_3 = 0. \tag{10}$$

Any two independent $\pm\boldsymbol{b}_k$ define a unit cell of the hexagonal lattice. If the hexagons in an hexagonal network surrounding a defect cluster are not arranged periodically, we may always define the vectors $\boldsymbol{b}_k$ at each hexagon after having defined their orientation at a particular hexagon. Each $\pm\boldsymbol{b}_k$ defines a neighbour of a particular hexagon.

We now consider an arbitrary six-belt of a defect with s hexagons (s (·)-vertices) and circulate around it clockwise, starting at hexagon 1. Associated with each six-belt hexagon we define a vector $\pm\boldsymbol{b}_k$ which is the vector between that hexagon and the previous one in a clockwise circuit. The vector associated with hexagon i will be denoted by $\boldsymbol{b}(i)$. We call $\boldsymbol{b}_1$ to the vector associated with the first hexagon ($\boldsymbol{b}(1) = \boldsymbol{b}_1$). The vectors $\boldsymbol{b}(i)$ associated with successive hexagons are obtained by rotating the antecedent $\boldsymbol{b}$ by $\Delta\theta_i$ given by

$$\Delta\theta_i = \frac{\pi}{3}(u_i - 1) \tag{11}$$

where u_i is the number of (o)-vertices preceding the (·) vertex u_i. (In a standard sequence u_i take values 1 or 2 only.) The sequence of $\pm\boldsymbol{b}_k$ vectors can then be obtained which ends at a vector $\boldsymbol{b}(s)$ having started with $\boldsymbol{b}(1) = \boldsymbol{b}_1$.

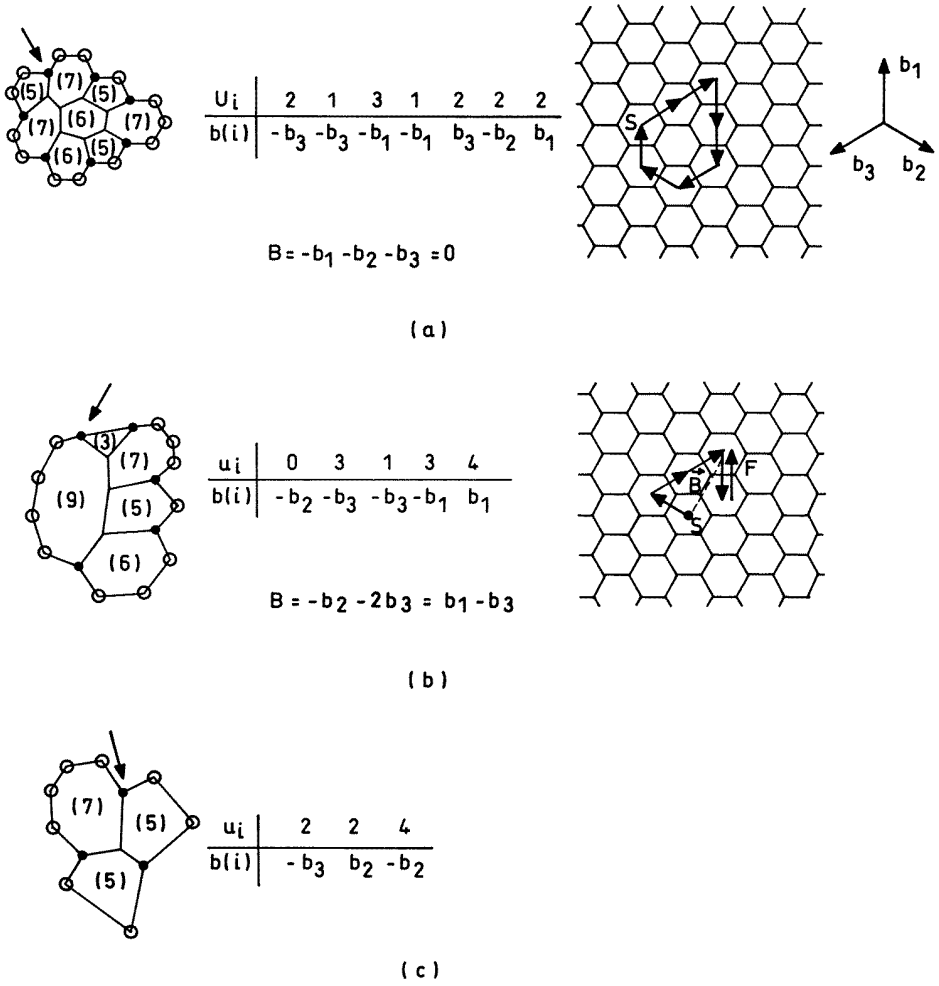

Figure 7. Examples of construction of $\boldsymbol{b}$-circuits associated with vertex sequences of defect clusters: (a) for a neutral defect; (b) for a dislocation defect, and (c) for a disclination defect. In (a) and (b) the circuit is redrawn in a perfect hexagonal network (starting point S; finishing point F). The three primitive vectors $\boldsymbol{b}_1$ $\boldsymbol{b}_2$ and $\boldsymbol{b}_3$ of the hexagonal lattice are shown at the top. All circuits have $\boldsymbol{b}(1) = \boldsymbol{b}_1$; (·)-vertex 1 is marked with an arrow.

The total rotation of the initial vector $\boldsymbol{b}_1$ or, equivalently, the angle between $\boldsymbol{b}(s)$ and $\boldsymbol{b}_1$ (rotation of $\boldsymbol{b}(s)$ to coincide with $\boldsymbol{b}_1$) is

$$\sum \Delta\theta_i = \frac{\pi}{3}\sum(1-u_i) = \frac{\pi}{3}(s-u) = 2\pi + \frac{\pi}{3}P \tag{12}$$

where the sum is over all the (·)-vertices (over all entries u_i) in the numerical vertex sequence.

If $P = 0$, the last vector $\boldsymbol{b}(s)$ coincides with $\boldsymbol{b}(1)$ (note that 2π is the sum of the turning angles in a closed polygonal circuit) and there is a one-to-one correspondence between (·)-vertices and $\boldsymbol{b}$-vectors in the sequence. The defect has no disclination character. If $P \neq 0$ the angle between $\boldsymbol{b}(s)$ and $\boldsymbol{b}(1)$ is $(\pi/3)P$. The defect has disclination character, the strength of the disclination being $(\pi/3)P$.

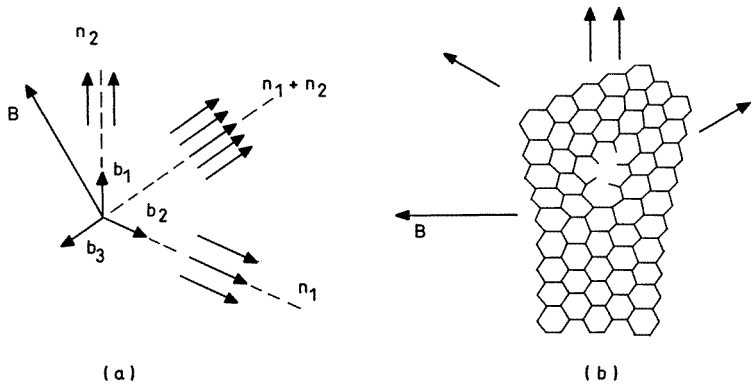

Figure 8. (a) Schematic illustration of the extra half-rows of hexagonal cells associated with a dislocation of Burgers vector $\boldsymbol{B} = n_1\boldsymbol{b}_1 - n_2\boldsymbol{b}_2$. (b) The hexagonal network for $\boldsymbol{B} = -\boldsymbol{b}_2 + \boldsymbol{b}_3$ with indication of the four extra half-rows.

When the $\boldsymbol{b}$-circuit of a defect with $P = 0$ is repeated in the perfect honeycomb it does not in general give a closed circuit. The finishing point F does not coincide with the starting point S. The defect is a dislocation with Burgers vector $\boldsymbol{B}$ defined as the vector SF. If F coincides with S it is $\boldsymbol{B} = 0$ and the defect is embeddable in a perfect honeycomb. It can be termed a neutral defect. In general

$$\boldsymbol{B} = \sum_{i=1}^{S} \boldsymbol{b}(i) \qquad P = 0 \tag{13}$$

where the sum is over all vectors $\boldsymbol{b}(i)$ of a $\boldsymbol{b}$-circuit.

The $\boldsymbol{b}$-circuit can be constructed based on any equivalent vertex sequence. Both the total rotation of $\boldsymbol{b}(1)$ and the Burgers vector (for $P = 0$) are invariant. In particular, one can use directly the vertex sequence of the cluster, with no need to consider any six-belt. In figure 7 we give examples of $\boldsymbol{b}$-circuits obtained directly from the vertex sequences of three defect clusters of each of the three main types of clusters. For $P = 0$, the $\boldsymbol{b}$-circuits are repeated in the perfect honeycomb (figures 7(a) and (b)).

The vector $\boldsymbol{B}$ of dislocation defects can be expressed in any vector basis, formed by two primitive vectors $\pm\boldsymbol{b}_k$. By conveniently choosing the primitive vectors $\boldsymbol{b}_k$ one can write the vector $\boldsymbol{B}$ in the form

$$\boldsymbol{B} = n_1\boldsymbol{b}_1 - n_2\boldsymbol{b}_2 \tag{14}$$

where $n_1 \geqslant n_2 \geqslant 0$ are the smallest possible $\boldsymbol{b}_k$ components of $\boldsymbol{B}$. The form (14) can easily be found by using (10). For example $\boldsymbol{B} = \boldsymbol{b}_1 + \boldsymbol{b}_2$ can be replaced by $\boldsymbol{B} = \boldsymbol{b}_1$. However, when dealing with more than one defect (e.g. interaction between defects) one must consider a unique basis and the $\boldsymbol{B}$ vectors may have other forms.

The hexagonal network surrounding a dislocation defect keeps its translational symmetry but contains extra half-rows of hexagons. It is easily found that for $\boldsymbol{B}$ in the form (14) the number of extra half-rows is $2(n_1 + n_2)$, with n_2 extra rows in direction 1, n_1 extra rows in direction -2 and $(n_1 + n_2)$ extra rows in direction -3, as schematically shown in figure 8(a). An example is given in figure 8(b) for a dislocation with $\boldsymbol{B} = \boldsymbol{b}_1 - \boldsymbol{b}_2$.

Finally we note that for $P \neq 0$, a $\boldsymbol{B}$ vector defined by (13) is dependent on the (equivalent) vertex sequence chosen. Therefore, for $P \neq 0$ the $\boldsymbol{b}$-circuit merely gives the strength of the disclination defect and $\boldsymbol{B}$ cannot be defined.

6. Minimal standard sequences and equivalence classes

Two equivalent clusters have equivalent vertex sequences and six-belts and can be embedded in an hexagonal network of given topology. The clusters can then be put in equivalence classes. In order to characterize the classes we indicate a standard vertex sequence for each. There are, however, infinitely many choices for a given class. We will choose what we term a minimal standard sequence, which is the one with the smallest number of vertices (i.e. with smaller numbers of entries 1 and 2). Since the number of entries 2 is fixed (equal to $P+6$), a minimal sequence is the standard sequence with minimum number of entries 1.

In the appendix we indicate how to obtain the minimal sequence from a given standard sequence and how to show that a sequence is minimal. Using the method described in the appendix we have identified all equivalence classes for each $P \geqslant -5$. The result is summarized in table 1. Examples of actual simple clusters (with at most two cells) are given in the table for a number of equivalence classes.

Table 1. Topological classes of defect clusters in hexagonal networks.

P	Minimal six-belt	Burgers vector	Simple clusters
-5	2 (12)	—	4/3
-4	22, 122	—	5/3; 4/4
-3	222, 1222	—	3; 4/5
-2	2222, 12222	—	4; 5/5; 3/7
-1	222222	—	5; 4/7; 3/8
0	$(1)^{n_1}\ 2(1)^{n_2}\ 22222$	$n_1\boldsymbol{b}_1 - n_2\boldsymbol{b}_2$	5/7; 4/8; 3/10 $(\boldsymbol{b}_1)$ $(\boldsymbol{b}_1 - \boldsymbol{b}_2)$ $(2\boldsymbol{b}_1)$[a]
1	2222222		7; 5/8; 4/9; 3/10
$1 < P \leqslant 5$	$22\ldots2$[b] and $122\ldots2$[b]		
6	$(1)^{n_1}\ 2(1)^{n_2}\ 2\ldots2$[c]	$n_1\boldsymbol{b}_1 - n_2\boldsymbol{b}_2$	

[a] Burgers vector of each cluster.
[b] $(P+6)$ sequence of 2.
[c] $(P+5)$ sequence of 2.

For $P = 0$ the defects are dislocations and can be classified in terms of the Burgers vector $\boldsymbol{B}$ which can take any form of type (14). The minimal sequence for a given pair n_1, n_2 in (14) can be written in the form

$$\begin{aligned} &\{(1)^{n_1}\ 2(1)^{n_2}\ 22222\} \\ &\boldsymbol{B} = n_1\boldsymbol{b}_1 - n_2\boldsymbol{b}_2 \end{aligned} \tag{14}$$

where $(1)^n$ indicates n successive entries 1.

For other P that are multiples of six (i.e. $P = 6k$, where k is an integer) there are infinitely many distinct vertex sequences of type (14) with the five successive entries 2 replaced by $5+6k$ entries 2. Although these defects (for $k \neq 0$) are disclinations, they can be identified by a vector $\boldsymbol{B}$, as for dislocations.

For each $P = 6k \pm 1$ (i.e. $P = -5, -1, 1, 5, 7, \ldots$) there is a unique equivalence class, with minimal sequence formed by $P+6$ entries 2

$$\{2\,2\,2\,2\ldots\}. \tag{15}$$

For $P = -5$ the minimal sequence {2} should be regarded as a formal representation of the defect; an equivalent sequence which can be realized with convex cells is {12}. Figure 9

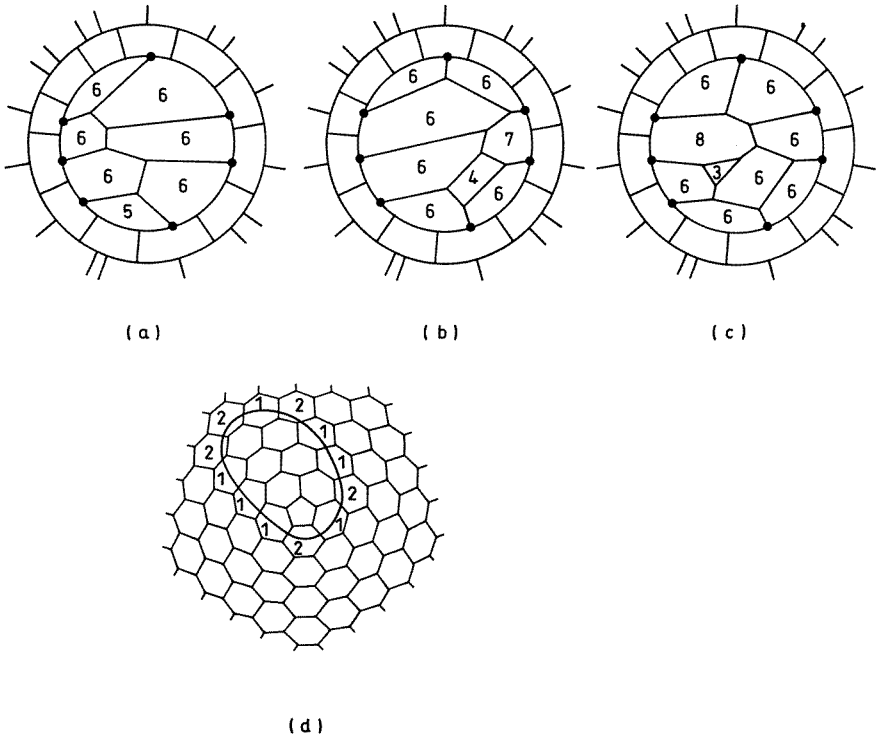

Figure 9. All defect clusters with $P = -1$ are equivalent. The figure shows how defects with one or two cells and $P = -1$ can be embedded in the same network. The defects are: (a) a five-cell; (b) a 4/7 pair and (c) a 3/8 pair. The common standard six-belt is redrawn in the network in (d) which is topologically identical to the one in (a).

shows the equivalence of clusters with $P = -1$ and one or two cells. For all these clusters with $P = -1$ a unique standard sequence can be found which is indicated in the figure.

Finally, for $P = 6k \pm 2$ and $P = 6k \pm 3$ there are two equivalent classes for each P, with minimal sequences containing zero or one entry 1

$$\{2\,2\,2\ldots2\}$$
$$\{1\,2\,2\,2\ldots2\}. \tag{16}$$

As discussed in the appendix, these two sequences are equivalent for $P = 6k \pm 1$.

7. Topological size number of a defect cluster

The short six-belt of a defect cluster contains s hexagons. This number then gives an indication of the topological size of a cluster, i.e. of its perimeter. If the defect is neutral ($P = 0$, $\boldsymbol{B} = 0$) the interior of the short six-belt can be filled with N hexagons, and this is another measure of the size of the defect, which we term the topological size number N. The actual area of the defect with N_c cells can of course be different from $N_c A_0$ where A_0 is the area of one hexagonal cell in the surrounding honeycomb.

To define a topological size number of a general defect cluster we proceed as follows. First, we transform the vertex sequence of the defect into a sequence with a minimum

number of vertices. To do this we use operations (5) and their reverse. The net number of hexagons that are placed inside the short six-belt can be path dependent, as shown in the example of figure 10. Let N_0 be the smallest net number. In the final vertex sequence the number of $(\cdot)$-vertices is s_m (in figure 10, $N_0 = 1$ and $s_m = 1$). Let N_1 be the integer following or equal to $(s_m + 1)$, then the size number of the defect is defined as

$$N = N_0 + N_1. \tag{17}$$

For example, an isolated cell with i sides ($i \neq 6$) has size number 1 ($N_1 = 1$) and a pair of $5/7$ cells has size number 2 ($N_1 = 2$). The change in size number is a convenient measure of the number of cells invaded by a defect that grows into a honeycomb froth [5].

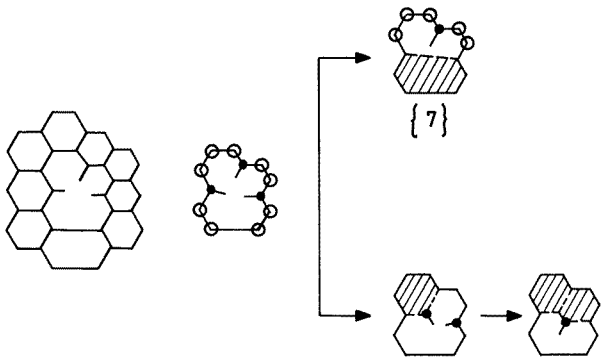

Figure 10. The number of hexagonal cells that is introduced inside a six-belt is path dependent. In the example, the minimum number of hexagons inserted is $N_0 = 1$.

8. Strain field and strain energy of defects

The hexagonal network around a defect cluster is in general distorted relative to the perfect honeycomb. This is due to the topological changes caused by the defect and also by the change of area resulting from the introduction of the defect.

We first assume that the change of area is zero (topological defect). For a neutral defect this will mean that the area inside a six-belt is the same as in the perfect honeycomb. For dislocation or disclination defects, the definition of the excess area of a cluster can be given in terms of the topological size of the cluster, N. The excess area, ΔA, is the difference between the actual area inside the cluster short six-belt and NA_0, where A_0 is the area of a cell in the honeycomb.

We treat the honeycomb as a 2D elastic isotropic continuum with Young's modulus E and shear modulus G. The Poisson's ratio is

$$\upsilon = \frac{E}{2G} - 1. \tag{18}$$

It will be assumed in the following that the 2D medium is incompressible; then $\upsilon = 1$ and $E = 4G$. A particularly important case is that of a 2D honeycomb froth, for which

$$G = \frac{1}{2\sqrt{3}}\frac{\gamma}{a_0} \tag{19}$$

where a_0 is the edge length ($A_0 = (3\sqrt{3}/2)a_0^2$) and γ is the film tension [10, 13].

For a dislocation defect we can use the well known equations for the elastic strain field of an edge dislocation at a fairly large distance r from the defect. Using polar coordinates (r, θ, with $\theta = 0$ in the direction of $\boldsymbol{B}$), the strain components for an incompressible 3D medium ($\upsilon = 1/2$) are (e.g. [14])

$$\varepsilon_{rr} = \varepsilon_{\theta\theta} = 0 \qquad \varepsilon_{r\theta} = \frac{B}{2\pi}\frac{\cos\theta}{r}. \tag{20}$$

These are also the strain components of the elastic field due to a dislocation in an incompressible 2D medium ($\varepsilon_{zz} = 0$). The average (over θ) strain energy density at a distance r is

$$\omega = \frac{G}{4\pi^2}B^2\frac{1}{r^2}. \tag{21}$$

This is an energy per unit volume, that is, per unit area of the 2D honeycomb and unit length perpendicular to it. The average energy density decreases with r^{-2} which is a consequence of the r^{-1} dependence of strain (and stress). For $\boldsymbol{B}$ given by equation (13) we have

$$B^2 = n_1^2 + n_2^2 + n_1 n_2 \qquad (n_1, n_2 \geqslant 0). \tag{22}$$

The strain field of a disclination cluster can be calculated as follows. The arrangement of six-cells around the cluster, centred at zero, can be obtained from the arrangement of the cells in a perfect honeycomb by inserting (for $P > 0$) or removing (for $P < 0$) a wedge of hexagonal cells of angle $P\pi/3$ centred at zero (see, for example [11]) as schematically shown in figure 11 for $P = +1$. This is because the number of six-cells in successive six-belts around the cluster increases by $P + 6$ as one goes from one six-belt to the next (outer) belt, while that number increases by six in the reference, hexagonal network.

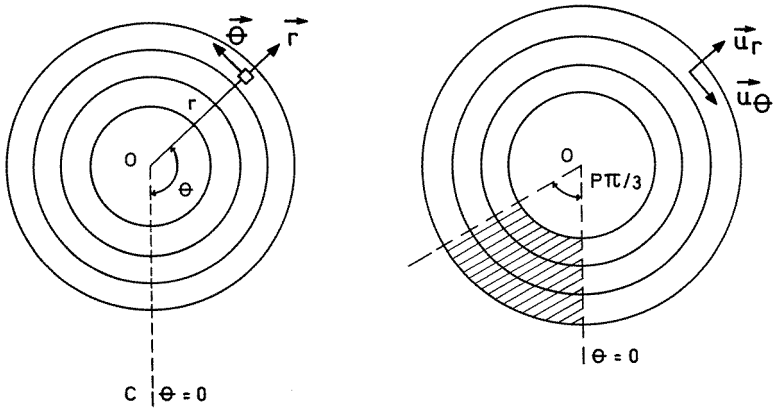

Figure 11. The arrangement of cells in the hexagonal network around a disclination cluster is obtained from that in a perfect honeycomb (a) by introducing a wedge of hexagonal cells of angular width $P(\pi/3)$ at a radial cut (C) in the honeycomb. The displacement $\boldsymbol{u}$ in polar coordinates (r, θ) has components $\boldsymbol{u}_r$, $\boldsymbol{u}_\theta$. The figure is drawn for $P = 1$.

The displacement field $\boldsymbol{u}$ associated with the disclination cluster is the strain field caused by the insertion/removal of the wedge. Using polar coordinates (r, θ) (figure 11), the radial component u_r of the displacement can easily be found assuming that the medium is incompressible. When the wedge is introduced, the change $u_r = \Delta r$ in r of a point in the honeycomb is given by

$$\Delta(\pi r^2) = P\frac{\pi}{6}r^2. \tag{23}$$

Then

$$u_r = \frac{P}{12}r. \tag{24}$$

This immediately gives

$$\varepsilon_{rr} = \frac{\partial u_r}{\partial r} = \frac{P}{12}. \tag{25}$$

Since the strain field is radially symmetric, the principal directions of strain are the radial ($\boldsymbol{r}$) and tangential (θ) directions and

$$\varepsilon_{r\theta} = 0. \tag{26}$$

Also, because of the assumed incompressibility, we have

$$\varepsilon_{\theta\theta} = -\varepsilon_{rr} = -\frac{P}{12}. \tag{27}$$

This can also be obtained directly from the tangential component of the displacement u_θ which is given by

$$u_\theta = -\frac{P}{6}r\theta \tag{28}$$

where θ is the angular polar coordinate relative to a reference direction $\theta = 0$ where $u_\theta = 0$ (θ is in the direction of increasing θ).

The strain energy density ω of a disclination cluster of strength P in an incompressible hexagonal network is then

$$\omega = \frac{1}{2}E(\varepsilon_{rr}^{\varepsilon} + \varepsilon_{\theta\theta}^2) = \frac{G}{36}P^2 \tag{29}$$

proportional to P^2 and independent of r.

The equations written above for the strain field of a 2D disclination assume an indefinite medium and differ from those derived by Timoshenko [15], for a 3D (wedge) disclination at the axis of a hollow finite cylinder.

The strain field of a geometrical defect of excess area ΔA in an incompressible honeycomb also has radial symmetry. The change $u_r = \Delta r$ of the distance r to the defect is simply obtained from

$$\Delta(\pi r^2) = \Delta A \tag{30}$$

or

$$u_r = \frac{\Delta A}{2\pi r}. \tag{31}$$

The components of strain are then

$$\varepsilon_{rr} = -\varepsilon_{\theta\theta} = -\frac{(\Delta A)^2}{2\pi r^2} \qquad \varepsilon_{r\theta} = 0 \tag{32}$$

and the strain energy density is

$$\omega = G\frac{(\Delta A)^2}{2\pi^2 r^4}. \tag{33}$$

9. Summary

Defect clusters in hexagonal networks can be topologically characterized by the sequence of two-connected and three-connected vertices (respectively (o)-vertices and (·)-vertices) at their periphery. The vertex sequence determines the type of hexagonal network in which the cluster is embedded.

Three main types of clusters can be identified, depending on the strength P of the cluster, defined as the difference between the total number of edges in the cluster and $6N_c$, where N_c is the number of cells forming the cluster. For $P \neq 0$ the cluster has disclination character and the hexagons around the cluster are rotated. For $P = 0$, the cluster type depends on its Burgers vector, which can also be determined from the vertex sequence. For $\boldsymbol{B} = 0$ the cluster is neutral and the hexagonal network around the cluster is perfect. For $\boldsymbol{B} \neq 0$ the network is dislocated and contains extra half-rows of hexagonal cells. For $P = 0$ (and also for $P = 6k$) there are infinitely many classes of clusters, each characterized by a vector $\boldsymbol{B}$. For $P \neq 0$ (and $P \neq 6k$), there are at most two classes for each P, each with a specific arrangement of the hexagons around the cluster. In general, the classes can be identified by particular vertex sequences (minimal sequences) which have been enumerated.

Given an arbitrary cluster of connected cells, it may not be possible to embed it in an hexagonal network. The conditions under which the cluster can be on embedded were enunciated in terms of properties of the vertex sequence. In particular, the strength of the cluster P must exceed -6.

If the area of a cluster of cells in an hexagonal network differs by ΔA from the area of N_c hexagonal cells (N_c is the number of cells in the cluster) there is a geometrical defect which in general adds to the topological defect.

Topological and/or geometrical defects induce strain in the surrounding hexagonal network. The strain field of disclination defects was evaluated using an elastic continuum approach for the surrounding network and admitting a strain field with radial symmetry. A similar calculation was done for purely geometrical defects. For dislocations we used well known results related to their strain field. While the strain (and stress) field of a dislocation defect decreases with r^{-1} (r is the distance to the defect), the strain field of a geometrical defect decreases with r^{-2} and that of disclination is independent of r. As a result, the strain energy density of a disclination cluster is a constant independent of r and proportional to P^2 (equation (29)), the strain energy of a dislocation cluster decreases with r^{-2} and is proportional to $\boldsymbol{B}^2$ (equation (21)) and the strain energy of a geometrical defect cluster decreases with r^{-4} and is proportional to $(\Delta A)^2$ (equation (33)).

Appendix. Minimal vertex sequences

Given a standard vertex sequence it is possible, by means of relatively simple rules, to obtain other equivalent, standard sequences which determine the same arrangement of the hexagons in the surrounding network. These operations change the number and location of entries 1 in the vertex sequence but leave the number of 2 unchanged. For defects with $P = 0$ (dislocations) the operations also leave invariant the Burgers vector. The rules that we indicate here are in fact obtained from the product of operations (5), such that only standard six-belts are obtained.

The basic rule relates the vertex sequences in two successive (adjacent) standard six-belts. The sequence of the outer six-belt is obtained from the one of the inner six-belt by introducing an extra entry 1 between successive 2, as in

$$12211212 \rightarrow 112121112112.$$

The reverse operation, when possible, allows a simplification of the vertex sequence.

The more general rule to be used is one to form a six-belt from a pair of adjacent (successive) six-belts. In the transformation one goes from one six-belt to the other and then returns to the original belt where the circuit is closed. The rule can be described by the following equations, where $(1)^n$ indicates a sequence of n entries 1 and (1,2) a sequence with at least one entry 2 (the dots indicate eventual additional entries which are unchanged)

$$\ldots 12\,(1)^n\,21\ldots \rightarrow \ldots 2\,(1)^{n+1}\,2\ldots$$
$$\ldots 12\,(1,2)\,21\ldots \rightarrow \ldots 2\,(1,2)\,2\ldots.$$

In the operations from left to right one goes from the outer to the inner six-belt, and *vice versa*.

In particular cases we have, for $n = 0$

$$1221 \rightarrow 212$$

and for $(1, 2) = 2$

$$12221 \rightarrow 222.$$

The minimal six-belts for each P are obtained by eliminating as many 1 as possible with the operations just indicated. For $P = 0$ the minimal sequences can be put in the general form

$$(1)^{n_1}\,2(1)^{n_2}\,22222 \tag{A1}$$

where $n_1 \geqslant n_2 \geqslant 0$ define the Burgers vector (see equation (14)). For example, in {12122222} no further 1 can be eliminated. Similar forms are obtained for $P = 6k$, with the 5 entries 2 replaced by $5 + P$ entries 2.

For $P \neq 6k$, all sequences can be reduced to one of the forms

$$\begin{aligned} &222\ldots 2 \\ &1222\ldots 2 \end{aligned} \tag{A2}$$

with $P+6$ successive 2. For $P = 6k \pm 1$ these two sequences are equivalent. For example, for $P = -1$.

$$\underset{}{22222} \quad \underset{\text{(Op2)}}{= 1222122} \quad \underset{\text{(Op1)}}{= 222212.}$$

For $P = 6k \pm 2$ or $P = 6k \pm 3$ the two sequences (A2) are not equivalent.

References

[1] Weaire D and Rivier N 1984 *Contemp. Phys.* **25** 59
[2] Levitan B 1994 *Phys. Rev. Lett.* **72** 4057
[3] Ruskin H J and Feng Y 1995 *J. Phys.: Condens. Matter* **7** L553
[4] Jiang Y, Mombach J and Glazier J 1995 *Phys. Rev.* E **52** R3333
[5] Vaz M Fátima and Fortes M A 1997 *J. Phys.: Condens. Matter* **9** 8921
[6] el Kader A A and Earnshaw J C 1997 *Phys. Rev.* E **56** 3251
[7] el Kader A A and Earnshaw J C 1997 *Phil. Mag.* A **76** 1251
[8] Prakash O, Bichebois P, Brechet Y, Louchet F and Embury J D 1996 *Phil. Mag.* A **73** 739
[9] Morral J E and Ashby M F 1974 *Acta Metall.* **22** 567
[10] Rosa M F and Fortes M A 1998 *Phil. Mag.* A **77** 1423
[11] Harris W F 1977 *Sci. Am.* **237** 130
[12] Fortes M A and Ferro A C 1985 *Acta Metall.* **33** 1697
[13] Khan S A and Amstrong R C 1986 *J. Rheology* **30** 409
[14] Nabarro F R N 1967 *Theory of Crystal Dislocations* (Oxford: Clarendon) ch 2
[15] Timoshenko S 1951 *Theory of Elasticity* (New York: McGraw-Hill)